

Challenges in Modelling and Optimization of Stability Constants in the Study of Metal Complexes with Monoprotonated Ligands

Part II

A Glass-Electrode Potentiometric and Polarographic Study of the Copper(II)/2-Hydroxy-3-[(2-hydroxy-1,1-dimethylethyl)amino]propane-1-sulfonic Acid (AMPSO)/Hydroxy System

by Carina M. M. Machado^{a)}, Ignacy Cukrowski^{*b)}, and Helena M. V. M. Soares^{*a)}

^{a)} REQUIMTE, Department of Chemical Engineering, Faculty of Engineering, University of Porto, Rua Dr. Roberto Frias, P-4200-465 Porto, Portugal (phone: 351-225081650; fax: 351-225081449; e-mail: hsoares@fe.up.pt)

^{b)} Molecular Sciences Institute, School of Chemistry, University of the Witwatersrand, P. O. Wits, Johannesburg 2050, South Africa (e-mail: ignacy@aurum.wits.ac.za)

The influence of 2-hydroxy-3-[(2-hydroxy-1,1-dimethylethyl)amino]propane-1-sulfonic acid (AMPSO = HL) on systems containing copper(II) was studied by glass-electrode potentiometry (GEP) and direct-current polarography (DCP), at fixed total-ligand-to-total-metal-concentration ratios and various pH values (25°, 0.1M KNO₃ medium). The predicted model ([CuL]⁺, [CuL(OH)]⁰, [CuL₂]⁰, [CuL₂(OH)]⁻, [CuL₂(OH)₂]²⁻, and [CuL₃]⁻) and the overall stability constants for species found were obtained by combining results from both electrochemical techniques. The last five complexes are reported for the first time. For the species [CuL]⁺, [CuL₂]⁰, [CuL₃]⁻, and [CuL₂(OH)₂]²⁻, it was possible to determine stability constants with reasonable certainty and their values, as log β, were found to be 4.62 ± 0.04, 9.5 ± 0.1, 13.4 ± 0.1, and 21.2 ± 0.1, respectively. For the species [CuL(OH)]⁰ and [CuL₂(OH)]⁻, stability constants 11.7 ± 0.2 and 15.6 ± 0.2, respectively, are presented as indicative values. It was demonstrated that AMPSO buffer may decrease the Cu²⁺ concentration by ten orders of magnitude by forming complexes with Cu²⁺. For the first time, the correction in DCP waves for the adsorption of the ligand and quasi-reversibility of the metal allowed to determine stability-constant values that are in good agreement with the values obtained by GEP. The importance of graphic analysis of data and significance of employing two analytical techniques was demonstrated; neither GEP nor DCP would be able to provide the correct M/L/OH⁻ model and reliable stability constants when used independently.

1. Introduction. – In the last three decades, Good and co-workers have synthesized several hydrogen-ion buffers for biological research [1][2]. These buffers were designed several criteria taken into account, including: *i*) they should have maximum water solubility and minimum solubility in other solvents to keep them from accumulating in the biological phase and preventing of passing through the membranes; *ii*) there should be a minimal effect of temperature and ionic strength on their pK_a values; *iii*) the buffers should be stable and must not absorb light of wavelengths above 240 nm; *iv*) they should be easy to prepare and inexpensive; *v*) they should not form complexes with cations, or, if they do, the complexes should be soluble, and their stability constants should be known [1][2].

In fact, some zwitterionic N-substituted aminosulfonic acids do not complex cations, as it was already demonstrated previously [3–6]. However, there are other

buffers, such as 2-hydroxy-3-[[2-hydroxy-1,1-bis(hydroxymethyl)ethyl]amino]propane-1-sulfonic acid (TAPSO), that form several complexes with Cu^{2+} [7]. AMPSO has a structure similar to that of TAPSO, and one might also expect that strong Cu-complexes of this buffer would be formed when AMPSO is used to control the pH. Both compounds, TAPSO and AMPSO, are commercially available (*e.g.*, from *Sigma-Aldrich*) as biological buffers. However, besides their $\text{p}K_{\text{a}}$ values, no information is provided on their complexing abilities with, *e.g.*, biologically important metal ions.

In this work, we report the overall stability constants for species formed in the $\text{Cu}^{2+}/\text{AMPSO}/\text{OH}^-$ system at 25° and ionic strength 0.1M KNO_3 . Three electrochemical techniques, direct-current polarography (DCP), differential-pulse polarography (DPP), and glass-electrode potentiometry (GEP), were employed. Five new complexes of Cu^{2+} with AMPSO were identified. Experiments by alternating-current polarography (ACP) were also carried out to check buffer adsorption at the Hg-working-electrode surface, under the experimental conditions used. A simple correction in DCP waves (for the adsorption of the ligand and quasi-reversibility of the electrochemical reduction of the metal ion) was successfully applied in the determination of stability constants.

2. Experimental. – 2.1. *Materials and Reagents.* The laboratory plastic- and glassware was conditioned in 0.5M HNO_3 and rinsed several times with dist. H_2O . All solns. were prepared with pure H_2O obtained by passing dist. H_2O through a *MilliQ*-water-purification system from *Millipore* (Bedford, MA, USA). A stock soln. of *ca.* 0.1M KOH was prepared from solid reagent (*Merck*, Darmstadt, Germany) and standardized with potassium hydrogen phthalate by potentiometric titration. The determination of carbonates as well as the exact concentration of the base soln. was done by the *Gran*-plot method [8]. A *ca.* 0.1M HNO_3 stock soln. was prepared from the concentrated acid (*Merck*) and standardized against the standard KOH soln. The ligand AMPSO (= HL; 99.1%) was obtained from *Sigma-Aldrich* (St Louis, Missouri, USA) and used as received. A $5 \cdot 10^{-2}$ M $\text{Cu}(\text{NO}_3)_2$ stock soln. (in $5 \cdot 10^{-3}$ M HNO_3) was prepared by dissolving a proper amount of an anal.-grade salt (*Merck*). The background electrolyte, KNO_3 (*Merck*), was used to adjust the ionic strength of all the solns. to 0.1M. In potentiometric studies, a *Merck* standard soln. of Cu^{2+} ($5.0 \cdot 10^{-2}$ M) was used. High-purity N_2 was used for deaeration of the sample solns.

2.2. *Instrumentation. Potentiometry.* The potentiometric (and polarographic) experiments were performed in a jacketed glass vessel from *Metrohm* (Herisau, Switzerland) with a magnetic stirrer and thermostatted at $25.0 \pm 0.1^\circ$ by a water bath. The titration data were collected by a PC-controlled system assembled with a *MicroBU-2030* micro burette from *Crison* (Barcelona, Spain) and a *MicroPH-2002* meter with a *Philips-GAH-110* glass electrode and an *90-02-00* double-junction reference electrode from *Orion* (Beverly, U.S.A.) with the outer chamber filled with background soln. (0.1M KNO_3). Automatic acquisition of data was done by means of a home-made program, COPOTISY.

Polarography. Polarographic measurements were performed with a computer-controlled instrumental setup [9] and a *663-VA* stand (*Metrohm*) equipped with a multimode electrode (*Metrohm*, model *6.1246.020*) as a working electrode, used in the dropping-Hg-electrode mode. A Ag/AgCl (3M KCl) electrode and a Pt electrode (both *Metrohm*) were used as reference and counter electrodes, respectively. The pH of the solns. was measured to ± 0.1 mV (± 0.001 pH units) with a *PHI-72* pH meter (*Beckman*) and a model *6.0733.100* Ag/AgCl (3M KCl) reference and a model *6.0133.100* glass electrode, both from *Metrohm*.

2.3. *Procedure. Alternating-Current Polarography (ACP).* ACP Experiments were run in the absence of the metal ion to evaluate the adsorption of the ligand on the surface of the Hg working electrode. The exper. conditions used were: amplitude of sinusoidal alternating current of 5 mV, frequency of 75 Hz, scan rate of 2.5 mV/s, and phase angle at 90° . The polarograms were scanned in the potential range between 0.2 and -1.2 V at three different pH values (8.0, 9.0, and 10.0), varying the ligand concentrations from $4.0 \cdot 10^{-4}$ to $1.3 \cdot 10^{-2}$ M. These pH values were chosen because they correspond to exper. conditions where AMPSO occurs as HL (100%), HL and L^- (50% of each), and L^- (100%), respectively. In this way, the adsorption of all forms of the ligand could be examined.

Glass-Electrode Potentiometry (GEP). Seven potentiometric titrations in the pH range between 3.2 and 11.0 (monotonic or dynamic titrant additions of KOH solns.) were performed to establish the model and determine the stability constants for the $\text{Cu}^{2+}/\text{AMPSO}/\text{OH}^-$ system. For each titration, between 70 and 200 points were collected. The Cu^{2+} concentration was kept at *ca.* $1 \cdot 10^{-3}$ M and the $[\text{L}_T]/[\text{M}_T]$ ratio of 9.1 was obtained by addition of an appropriate amount of the ligand AMPSO.

Direct-Current and Differential-Pulse Polarography (DCP and DPP, resp.). Two polarographic techniques (DC and DP) were simultaneously applied to the same soln. sample to evaluate the electrochemical behavior of the system $\text{Cu}^{2+}/\text{AMPSO}/\text{OH}^-$. A drop time of 2 s and a step potential of 4 mV were used for both techniques. In the DPP measurements, a pulse height of 50 mV was used, with pulse width and integration time of 200 ms and 60 ms, resp. A typical polarographic experiment consisted of the following steps: after a scan of the background soln. (a check for impurities), a proper amount of Cu^{2+} standard soln. was added to the cell, and another polarogram was recorded; the next step involved the addition of a certain amount of the solid ligand AMPSO, to obtain the required ligand-to-metal ratio, followed by a new scan; finally, the pH of the soln. sample was varied in small steps, usually in 0.1-pH units, between 2.8 and 10 by the addition of standardized base, and after each addition, a new polarogram was recorded. In this way, a set of between 40–60 polarograms (representing all the species present at each pH value) was recorded. Several different total-ligand-to-total-metal-ion concentration ratios ($[\text{L}_T]/[\text{M}_T]$) were used. For the $[\text{L}_T]/[\text{M}_T]$ ratios 155, 271, and 72, the total Cu^{2+} concentrations were $4.9 \cdot 10^{-5}$, $7.5 \cdot 10^{-6}$, and $1.5 \cdot 10^{-5}$ M, resp. The equilibrium of the metal/ligand solns. was tested, and it was reached in a few minutes.

Calibration of the Glass Electrode. The measurements of $\text{pH} = -\log_{10}[\text{H}^+]$ (for all techniques described above) were performed after the calibration of the glass electrode. This calibration was achieved by a potentiometric titration of nitric acid with potassium hydroxide (both standardized solutions). The values in E° and response slope were obtained by fitting a straight line to the experimental points collected around pH 2 and 11.

2.4. Data Treatment. AMPSO, a zwitterionic buffer, has two protonation constants; the first is due to the sulfonic group and the other involves the amino group. In a previous work [7], we determined the $\text{p}K_{a2}$ for a related zwitterionic buffer, 2-hydroxy-3-[[2-hydroxy-1,1-bis(hydroxymethyl)ethyl]amino]propane-1-sulfonic acid (TAPSO). In addition, it has been verified that the sulfonic group of TAPSO was already deprotonated below pH 3. The value of $\text{p}K_{a2}$ of TAPSO established by us in that work was in very good agreement with the values reported [10–13]. Therefore, in the case of AMPSO, we decided to use the literature $\text{p}K_{a2}$ value of 9.05 [14] determined for the exper. conditions as employed in this work (Table 1). The program ESTA [15] was used to analyze the potentiometric data. During the refinement operations, the K_w [16], the protonation constant for the ligand AMPSO [14], as well as the formation constants for the hydroxy copper species [16] were kept at fixed values as given in Table 1.

Table 1. Dissociation Constant for Water, Protonation Constant for the Ligand AMPSO, and Overall Stability Constants for Copper(II) Complexes with OH^- , at 25°

	Equilibrium	Log β	μ	Ref.
Water	$\text{H}^+ + \text{OH}^- \rightleftharpoons \text{H}_2\text{O}$	13.78	0.1	[16]
AMPSO	$\text{L}^- + \text{H}^+ \rightleftharpoons \text{HL}$	9.05	0.1	[14]
Copper(II)	$\text{Cu}^{2+} + \text{OH}^- \rightleftharpoons \text{Cu}(\text{OH})^+$	6.1	0.1	[16]
	$2\text{Cu}^{2+} + \text{OH}^- \rightleftharpoons \text{Cu}_2(\text{OH})^{3+}$	8.2	3.0	[16]
	$\text{Cu}^{2+} + 2\text{OH}^- \rightleftharpoons \text{Cu}(\text{OH})_2$	11.8	0.1	[16]
	$\text{Cu}^{2+} + 3\text{OH}^- \rightleftharpoons \text{Cu}(\text{OH})_3^-$	14.5	1.0	[16]
	$\text{Cu}^{2+} + 4\text{OH}^- \rightleftharpoons \text{Cu}(\text{OH})_4^{2-}$	15.6	1.0	[16]
	$2\text{Cu}^{2+} + 2\text{OH}^- \rightleftharpoons \text{Cu}_2(\text{OH})_2^{2+}$	16.8	0.1	[16]
	$3\text{Cu}^{2+} + 4\text{OH}^- \rightleftharpoons \text{Cu}_3(\text{OH})_4^{2+}$	33.5	0.1	[16]
	$\text{Cu}(\text{OH})_2(\text{s}) \rightleftharpoons \text{Cu}^{2+} + 2\text{OH}^-$	–18.48	0.7	[16]

The refinement of polarographic data was achieved by the *Cukrowski* method [17][18]; this method uses mass-balance equations written for a labile and reversible metal/ligand system studied at a fixed total-ligand-to-total-metal concentration ratio $[\text{L}_T]/[\text{M}_T]$ and varied pH. The model is refined by comparing exper. and calc. complex-formation curves for the labile (on the polarographic time scale) metal/ligand systems.

3. Results and Discussion. – 3.1. *Ligand Adsorption and Copper Reversibility Studies.* ACP at a phase angle of 90° was used to test whether there was adsorption of AMPSO at the Hg electrode. This phase angle was chosen because the current is then capacitive in nature and proportional to the double-layer capacity. The studies showed that there was a small but significant ligand activity (in the range of potential where Cu^{2+} is reduced) particularly at $[\text{L}_\text{T}]$ larger than $1.2 \cdot 10^{-3}$ M (data not shown).

Two polarographic experiments, with $[\text{L}_\text{T}]/[\text{M}_\text{T}]$ ratios of 271 and 155, involved the ligand concentration larger than $1.2 \cdot 10^{-3}$ M. Analysis of DC and DP polarograms obtained for these two $[\text{L}_\text{T}]/[\text{M}_\text{T}]$ ratios did not show a significant increase or decrease in the recorded current, but the shape of recorded waves and peaks varied significantly from expected curves. For instance, for the $[\text{L}_\text{T}]/[\text{M}_\text{T}]$ ratio of 155, the DPP peak width ($w_{1/2}$) and the gamma coefficient for DCP waves varied between 62 and 65.5 mV and between 0.9 and 0.6, respectively. These values indicated that the behavior of the system, besides the influence of adsorption, could be regarded as not fully reversible [19]. The refinement of polarographic data [17][18] employed in this work requires that the recorded curves must represent fully reversible electrochemical processes if accuracy in obtained stability constants is of interest. As far as we know, there is yet neither theory nor a suitable mathematical-data treatment that would allow a direct use of experimental results obtained from quasi-reversible electrochemical processes. It is known that the limiting diffusion current I_d does not depend on the degree of reversibility. Thus, we decided to use a simple procedure for correcting the departure from the reversibility of the DCP data, which is illustrated in *Fig. 1*. The DCP wave is a sigmoidal curve and can be reproduced by the set of *Eqns. 1–3*, where I_r , I_b and I_{obs} stand for the reduction, background, and observed total current, n stands for a number of electrons (here two), E_{appl} is the stepwise applied potential at which the total current was recorded, and γ is a coefficient describing how steep the polarographic wave is. Theoretically, if the process is fully reversible, then the γ coefficient should be equal to one. By fixing this coefficient at one and by keeping a sufficient number of experimental points (circles), it was possible to obtain the corrected limiting diffusion current, I_d , and half-wave potential, $E_{1/2}$, from the computed curves, as it is illustrated in *Fig. 1*. The number of experimental points allowed in the fitting operation was varied in such a way that the theoretically computed DC wave reproduced the background current (dotted lines in *Fig. 1*) and the current at the foot of the wave well, and the limiting current was parallel to the background current when going through experimental points obtained at significantly more-negative potential when compared with $E_{1/2}$. The above procedure was used to compute corrected I_d and $E_{1/2}$ for all DC polarograms. Attempts to correct DPP experimental curves as described elsewhere [20] were not successful. This shows that the DCP technique is by far a more-suitable technique to use in cases of M/L/OH⁻ systems that are not fully reversible.

$$I_r = I_d / (10^{(n\gamma(E_{\text{appl}} - E_{1/2}))/0.05916} + 1) \quad (1)$$

$$I_b = a + bE_{\text{appl}} \quad (2)$$

$$I_{\text{obs}} = I_r + I_b \quad (3)$$

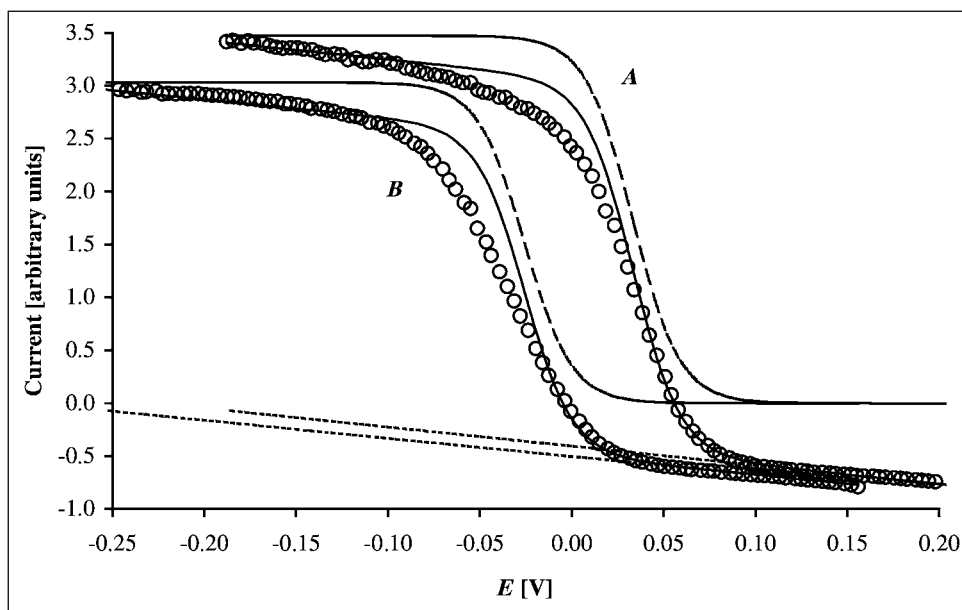


Fig. 1. Illustration of the fitting procedure of the DC polarograms. For details, see the text. A: $[\text{Cu}^{2+}] = 4.9 \cdot 10^{-5} \text{ M}$ in background solution, 0.1 M KNO_3 ; B: solution A after the addition of $7.5 \cdot 10^{-3} \text{ M}$ of the ligand AMPSO, adjusted to pH 6.60 by addition of KOH. Circles (\circ), experimental points; dotted lines (\cdots), computed background current, Eqn. 2; solid lines ($—$), computed DC curves for fully reversible process, Eqn. 3 (I_d and $E_{1/2}$ was used from those fitted curves in the computation of stability constants); dashed lines ($- - -$), computed reduction current for fully reversible process, Eqn. 1.

3.2. *Modelling Procedures and Refinement of Stability Constants.* Prior to any refinement operation, a reasonable M/L/OH^- model and suitable guesses in the stability constants for the proposed complexes must be prepared. Evaluation of the GEP data was performed with the ESTA program [15]. Values of the complex-formation function Z_M , defined elsewhere [21], were calculated for each datum point. The analysis of the Z_M function, represented in Fig. 2 for one titration and a selected M/L model as an example, is a helpful tool to understand the system as it allows to predict the formation of some complex species just by graphic analysis. The analysis of the Z_M function clearly indicates the formation of $[\text{CuL}_2]$ and $[\text{CuL}_3]^-$ as the major metal-containing species because the Z_M function shows typical and stepwise sigmoid increase to the value of 3. Above the value of 3, the Z_M function shows a typical feature (back-fanning) for the formation of major species containing OH ligands. The formation of the $[\text{CuL}]^+$ complex as a major species is not seen in Fig. 2; the Z_M function continuously increases from 0 to 2 without showing a plateau at the value of 1. If the complex $[\text{ML}]^+$ is formed, then its formation is immediately followed by the formation of $[\text{ML}_2]$ ($[\text{ML}]^+$ must be then a minor metal-containing species). It is important to stress that the Z_M function can be generated only for the assumed M/L/OH^- model. This implies that one has to investigate numerous possible models and generate Z_M

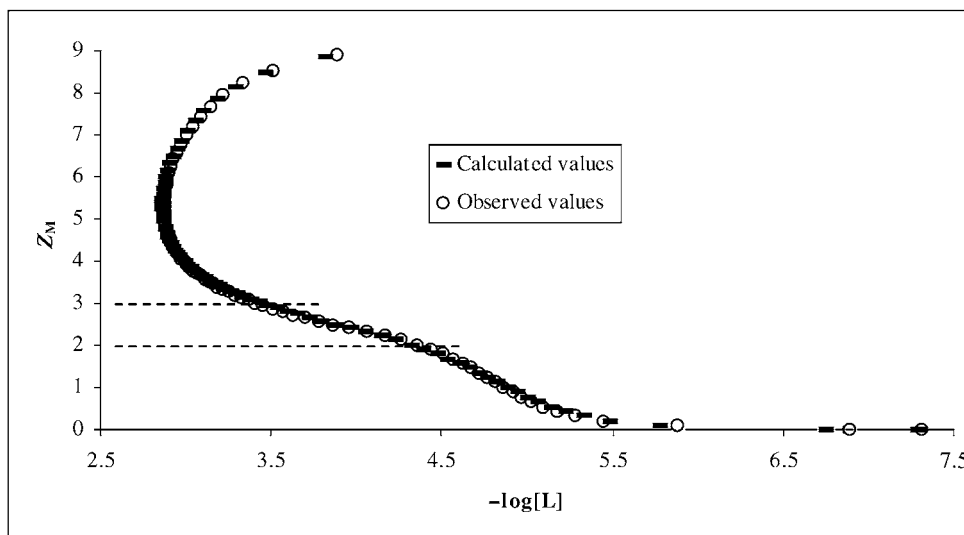
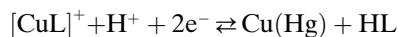


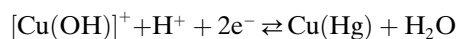
Fig. 2. Z_M Function calculated from the refinement operations performed on the GEP data by the program ESTA. The computed Z_M function was obtained for $[\text{CuL}]^+$, $[\text{CuL}_2]$, $[\text{CuL}_3]^-$, and $[\text{CuL}_2(\text{OH})_2]^{2-}$ (Model 1 in Table 2). $[\text{L}_1]/[\text{M}_1] = 9.1$; $[\text{M}_1] = 8.97 \cdot 10^{-4} \text{ M}$, at 25° and 0.1M KNO_3 .

functions for all of them to select the most probable one, usually based on the observed fit of the theoretical function with the objective (experimental) one.

The analysis of several DCP titrations, performed at different ligand-to-metal ratios in a pH range between 2.8 and 10, showed only one DCP wave. This wave shifted towards more cathodic potential and represents all labile metal-containing species $[\text{Cu}_p(\text{AMPSO})_x(\text{OH})_y]$ present in the solution. The direct graphic analysis of the experimental DCP data corroborated the information obtained from GEP data. From the analysis of the shift in $E_{1/2}$ vs. pH (Fig. 3, a), it is seen that there is no slope of 30 mV per pH unit; this slope is characteristic for a two-electron reduction process at the dropping-Hg electrode involving one proton, *i.e.*,

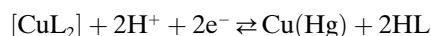


or/and

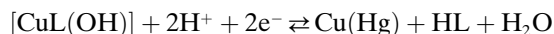


This supports the conclusion arrived at from the analysis of the GEP results, that if the complex $[\text{CuL}]^+$ is formed, then it is only to a small extent. It is important to mention that the formation of $[\text{Cu}(\text{OH})]^+$ must not be rejected from the overall M/L model as this is the pH range where its formation is, indeed, expected.

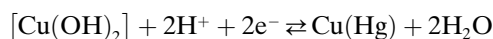
A slope of 59 mV per pH is observed throughout more than one pH unit – see the points in the pH range between 6.5 and 7.5 in *Fig. 3, a*. This clearly indicates the formation of $[\text{CuL}_2]$ or $[\text{CuL}(\text{OH})]$ species according to electrochemical reactions involving two protons, *i.e.*,



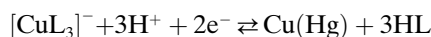
or/and



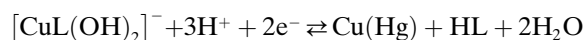
In principle, one must also consider the formation of $[\text{Cu}(\text{OH})_2]$, the reduction of which also would involve two protons, *i.e.*,



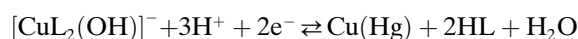
In the pH range between 7.5 and 9.0, an increase in the slope from 59 to 77 mV per pH unit was observed, suggesting the formation of $[\text{CuL}_3]^-$, $[\text{CuL}(\text{OH})_2]^-$, or $[\text{CuL}_2(\text{OH})]^-$ according to the electrochemical reactions involving three protons, *i.e.*,



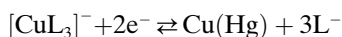
or/and



or/and



The theoretically expected slope when three protons are involved is *ca.* 90 mV. The experimental slope did not reach the theoretical value of 90 mV/pH because the protonation constant of the ligand AMPSO is *ca.* 9, and electrochemical processes without involvement of protons must also take place, *e.g.*,



hence, the observed slope is a resultant slope caused by numerous electrochemical reactions where, on average, the number of protons involved is between two and three. Note that, in the electrochemical reaction at the dropping-Hg electrode involving three protons, one has also to consider the formation of $[\text{Cu}(\text{OH})_3]$.

Above pH 9, the ligand is mainly in the deprotonated form L^- . The observed decrease in the slope from 77 (in the pH range below $\text{p}K_{\text{a}2}$) to 70 mV per pH unit (above $\text{p}K_{\text{a}2}$) fully confirms the formation of species $[\text{CuL}_x(\text{OH})_y]$. If one assumes that

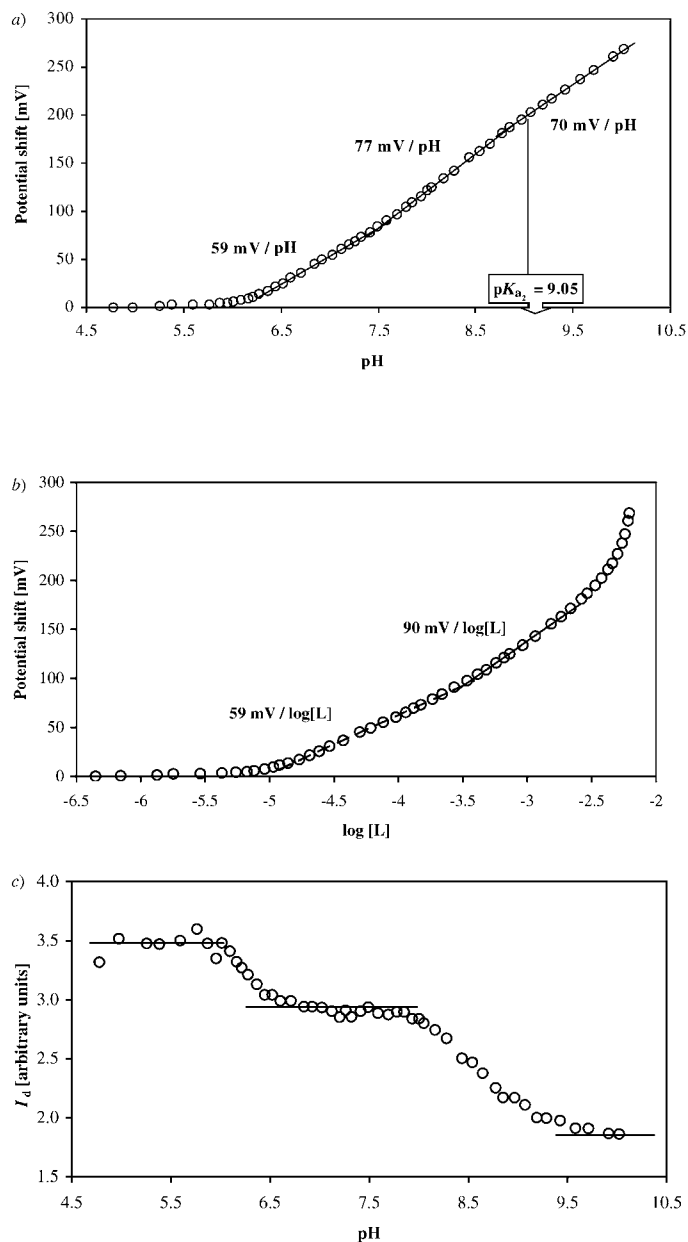
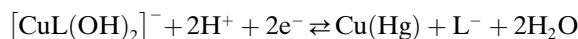
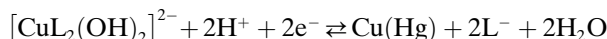


Fig. 3. Analysis of the DCP data obtained from the $\text{Cu}^{2+}/\text{AMPSO}/\text{OH}^-$ system at 25° and 0.1M KNO_3 ionic strength: a) Shift in the corrected half-wave potential as function of pH; b) shift in the corrected half-wave potential vs. the computed free-ligand concentration; c) variation in I_d (obtained after correction shown in Fig. 1) vs. pH. $[\text{L}_T]/[\text{M}_T] = 155$, $[\text{M}_T] = 4.9 \cdot 10^{-5}$ M.

$[\text{Cu}_x(\text{OH})_y]$ were solely present throughout the experiment, then a continuous increase in the slope would be observed with an increase in the pH. This increase in the slope would be due to the consecutive increase in the number of OH ligands involved in the complex formation. In addition, precipitation of $\text{Cu}(\text{OH})_2(\text{s})$ would be expected, and that was not observed. In other words, the decrease in the slope at $\text{pH} \approx \text{p}K_{\text{a}2}$ could only be explained if the ligand was involved in the complex formation reaction with the metal ion throughout the whole pH range. The observed slope of 70 mV confirmed the formation of $[\text{CuL}_x(\text{OH})_2]$ species, such as



or/and



It is important to realize that, in the pH range above the $\text{p}K_{\text{a}2}$ value (where mainly L^- exists), the experimental slope depends only on the number of OH ligands involved in the complex-formation reaction. This means that one is unable to establish the number of L involved in the complex-formation reaction from the relationship seen in *Fig. 3, a*. The theoretically expected slope of 60 mV might mean the formation of $[\text{ML}(\text{OH})_2]^-$, $[\text{ML}_2(\text{OH})_2]^{2-}$, ... $[\text{ML}_x(\text{OH})_2]^{x-}$, all of which contain two OH ligands.

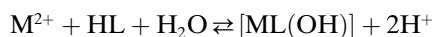
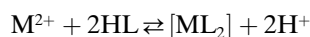
From the above, it is obvious that additional information is required to suggest a most likely model, particularly at high pH values. The analysis of the graph $E_{1/2}$ vs. $\log [\text{L}]$ (*Fig. 3, b*) is used to confirm the formation of $[\text{M}_p\text{L}_q]$ species [17]. Once again, there was no evidence of $[\text{CuL}]^+$ formation (no slope of 30 mV was identified). The well-defined slopes of 59 and 90 mV confirmed unequivocally the formation of $[\text{CuL}_2]$ and $[\text{CuL}_3]^-$, respectively, as major species present in solution. Now it has become clear that the large shift, if not the largest shift reported to date from the polarographic studies of metal complexes, observed in *Fig. 3, a*, cannot be attributed only to the formation of $[\text{Cu}_x(\text{OH})_y]$. As a matter of fact, all the above indicates that the species $[\text{Cu}_x(\text{OH})_y]$ are not formed to a large extent in the pH range investigated in this study.

In *Fig. 3, c*, the I_d determined after the correction shown in *Fig. 1* was plotted against the pH of the solution. Three regions can be distinguished: *i*) up to $\text{pH} \text{ ca. } 6$, where I_d remained at the level recorded for the metal-ion solution, indicating that significant amounts of complexes with the ligand AMPSO was not formed; *ii*) a well-defined pH region between 6.4 and 7.8, where I_d had very much the same value indicating the formation of a major species in the solution (perhaps $[\text{CuL}_2]$ as $[\text{ML}]^+$ was excluded as a major solution component); *iii*) above pH of *ca. 7.8*, a decrease in I_d was observed indicating the formation of consecutive species like $[\text{ML}_3]^-$, $[\text{ML}_x(\text{OH})_2]^{x-}$, etc. The recorded current seems to asymptotically approach a constant value above pH 9.5 suggesting the presence of another predominant species there, possibly $[\text{CuL}_2(\text{OH})_2]^{2-}$, if the above discussion and analyses of slopes shown in *Fig. 3, a*, are taken into consideration.

From the above, it was possible to propose the most likely M/L model that included $[\text{CuL}]^+$ (possibly), $[\text{CuL}_2]$, $[\text{CuL}_3]^-$, and $[\text{CuL}_x(\text{OH})_2]^{x-}$, where x most likely stands

for 1 and 2. To establish a sequence in the formation of complexes, one also should include $[\text{CuL}_x(\text{OH})]^{(x-1)-}$ in the overall initial model that consisted of $[\text{ML}]^+$, $[\text{ML}_2]$, $[\text{ML}_3]^-$, $[\text{ML}(\text{OH})]$, $[\text{ML}(\text{OH})_2]^-$, $[\text{ML}_2(\text{OH})]^-$, and $[\text{ML}_2(\text{OH})_2]^{2-}$ plus all known $[\text{Cu}_x(\text{OH})_y]$ species.

The next step was to refine the GEP data with the program ESTA. It immediately appeared that ESTA was able to refine several different models with refined stability constants in a wide range for the same species. The overall statistical parameter, the R factor, did not provide enough information on rejection or acceptance of a particular model. It became obvious that a special strategy had to be developed to propose a final M/L/OH^- model. The strategy, as well as the results obtained, are illustrated in *Table 2*. Note that all refinement operations were carried out without the simultaneous optimization of analytical parameters, such as $[\text{H}]$, $[\text{L}]$, or E° . First, we started by including in the M/L/OH^- model all seven $[\text{ML}_x(\text{OH})_y]$ complexes mentioned above. The program ESTA always rejected $[\text{CuL}(\text{OH})_2]^-$ and $[\text{CuL}_2(\text{OH})]^-$, regardless of the initial values in the stability constants. After removing these two complexes from the model, the program ESTA was randomly rejecting either $[\text{ML}(\text{OH})]$ or $[\text{ML}_2]$, converging to either *Model 1* ($[\text{ML}]^+$, $[\text{ML}_2]$, $[\text{ML}_3]^-$, and $[\text{ML}_2(\text{OH})_2]^{2-}$), or *Model 2* ($[\text{ML}]^+$, $[\text{ML}_3]^-$, $[\text{ML}(\text{OH})]$, and $[\text{ML}_2(\text{OH})_2]^{2-}$) (see *Table 2*). This strongly indicated that ESTA was not able to distinguish between $[\text{ML}_2]$ and $[\text{ML}(\text{OH})]$. One must realize that the formation of these two complexes occurs in the pH range where HL is the major form of the ligand (*Fig. 4*), and it involves the same amount of protons



The statistical data treatment (refinement) involving $[\text{ML}_2]$ illustrates the difficulties in making final decisions based only on mathematical operations, *e.g.*, based only on the R factor; one could easily propose a model without the complex $[\text{ML}_2]$. However, the rejection of $[\text{CuL}_2]$ is not supported by the graphical analysis of the Z_M function (*Fig. 2*) and by DCP data (slope of 59 mV as shown in *Fig. 3, b*). The complex $[\text{CuL}_2]$ is unequivocally present in solution. After fixing one of these complexes ($[\text{ML}(\text{OH})]$ or $[\text{ML}_2]$), the program ESTA was able to refine the other stability constant (*Models 3–5* in *Table 2*).

The program ESTA always accepted $[\text{CuL}_3]^-$ and $[\text{CuL}_2(\text{OH})_2]^{2-}$, regardless of the presence of other complexes included in the model. The refined stability constants for these two complexes, as $\log \beta$, were 13.53 ± 0.04 and 21.35 ± 0.02 , respectively (note that the standard deviations indicate here the ranges in stability-constant values obtained from different refined models). The refinement operations performed on potentiometric data suggest that $[\text{CuL}_3]^-$ and $[\text{CuL}_2(\text{OH})_2]^{2-}$ are the most-stable Cu^{2+} complexes formed with the ligand AMPSO. This can be used as a strong support for the supposition that these two complexes, $[\text{CuL}_3]^-$ and $[\text{CuL}_2(\text{OH})_2]^{2-}$, are octahedral and that the ligand AMPSO acts here as a didentate ligand with the N-atom and one alcoholic O-atom as donor atoms involved in the bonds with Cu^{2+} .

Table 2. Overall Stability Constants for the $\text{Cu}^{2+}/\text{AMPPO}/\text{OH}^-$ System Refined with the ESTA Program from GEP Data. $[\text{L}_\text{T}]/[\text{M}_\text{T}] = 9.1$; $[\text{M}_\text{T}] = 8.97 \cdot 10^{-4} \text{ M}$, at 25° and 0.1 M KNO_3 . Simultaneous refinement of data collected from four independent potentiometric titrations (762 points).

Complexes	Model 1	Model 2	Model 3	Model 4	Model 5	Model 6
$[\text{CuL}]^+$	4.60 ± 0.02	4.65 ± 0.02	4.61 ± 0.02	4.62 ± 0.02	4.63 ± 0.02	4.60 ± 0.02
$[\text{CuL}_2]$	9.69 ± 0.02	–	9.60 (fixed)	9.52 ± 0.02	9.28 ± 0.04	9.54 ± 0.02
$[\text{CuL}_3]^-$	13.54 ± 0.02	13.51 ± 0.02	13.54 ± 0.02	13.53 ± 0.02	13.52 ± 0.02	13.3 (fixed)
$[\text{CuL}(\text{OH})]$	–	12.23 ± 0.02	11.53 ± 0.07	11.7 (fixed)	12.0 (fixed)	11.7 (fixed)
$[\text{CuL}(\text{OH})_2]^-$	–	–	–	–	–	–
$[\text{CuL}_2(\text{OH})]^-$	–	–	–	–	–	15.52 ± 0.05
$[\text{CuL}_2(\text{OH})_2]^{2-}$	21.33 ± 0.02	21.35 ± 0.02	21.34 ± 0.02	21.33 ± 0.02	21.34 ± 0.02	21.32 ± 0.02
R-Factor	0.0145	0.0143	0.0145	0.0144	0.0143	0.0146

It was possible to refine the stability constants for the complex $[\text{CuL}_2(\text{OH})]^-$, but only when other complexes were kept fixed (see Model 6 in Table 2). As one can see in Fig. 2, with the model $[\text{CuL}]^+$, $[\text{CuL}_2]$, $[\text{CuL}_3]^-$, and $[\text{CuL}_2(\text{OH})_2]^{2-}$, an almost perfect fit was obtained between the calculated and the experimental values. A similarly good fit, however, was obtained when, e.g., $[\text{CuL}(\text{OH})]$ and $[\text{CuL}_2(\text{OH})]^-$ were included in the model (see Model 6 in Table 2). In this case, the analysis of the Z_M function generated for different models was of no help in deciding on the most likely and final M/L/OH⁻ model because the observed differences were not significant enough – very much the same R factor was obtained for all models shown in Table 2.

The refinement of the stability constant from the DCP data was performed by means of the experimental and calculated complex-formation curves [17]. Some of the refinement results are shown in Table 3. The results confirmed some observations and conclusions made from refinement of the GEP data. The complexes $[\text{CuL}_2]$, $[\text{CuL}_3]^-$, and $[\text{CuL}_2(\text{OH})_2]^{2-}$ appeared to be the most ‘favorite’ species throughout all the refinement operation; they had to be the major species in the solution (Model 1, Table 3) as predicted from the analysis of the experimental data shown in Fig. 3. The values of the stability constants obtained for $[\text{ML}_3]^-$ and $[\text{ML}_2(\text{OH})_2]^{2-}$, calculated from DCP experiments (Model 1, Table 3), were in good agreement with those refined from potentiometric titrations (Models 1 and 2, Table 2). These results show that, except for $[\text{ML}_2]$ (for more details see below), the correction performed for adsorption and the departure from reversibility was efficient. Moreover, $[\text{CuL}(\text{OH})_2]^-$ does not seem to form at any significant concentration since it was rejected by DCP and ESTA refinement operations; as a matter of fact, GEP and DCP showed that complex $[\text{ML}(\text{OH})_2]^-$ appeared to be the least likely species formed in a solution.

The analysis of the stability constants obtained by both electrochemical techniques, compiled in Tables 2 and 3, suggests some observations. Regarding the $\log K_{\text{CuL}}$, ESTA refined this value to 4.62 ± 0.04 (note that the standard deviation indicates here the ranges in stability-constant values obtained from different refined models). The DCP program was not able to give an estimate for this stability constant, the reasons being *i*) the large excess of $[\text{CuL}_2]$, *ii*) possibly not enough data points collected prior to the formation of $[\text{ML}_2]$, or *iii*) that the contribution brought by the experimental points related to the formation of $[\text{ML}]^+$ was not significant enough for the refinement operations. However, fixing $\log K_{\text{ML}}$ at the GEP or slightly lower value resulted in

Table 3. Overall Stability Constants for the $\text{Cu}^{2+}/\text{AMPSO}/\text{OH}^-$ System Obtained from DCP Data. At 25° and 0.1M KNO_3 , $[\text{L}_T]/[\text{M}_T] = 155$, $[\text{M}_T] = 4.9 \cdot 10^{-5}\text{ M}$.

Complexes	Model 1	Model 2
$[\text{CuL}]^+$	4.62 (fixed)	4.62 (fixed)
$[\text{CuL}_2]$	9.95 ± 0.02	9.95 ± 0.02
$[\text{CuL}_3]^-$	13.51 ± 0.02	13.3 ± 0.3
$[\text{CuL}(\text{OH})]$	–	–
$[\text{CuL}(\text{OH})_2]^-$	–	–
$[\text{CuL}_2(\text{OH})]^-$	–	15.7 ± 0.4
$[\text{CuL}_2(\text{OH})_2]^{2-}$	21.19 ± 0.01	21.16 ± 0.02
S.d. ($\pm \text{mV}$) ^{a)}	1.755	1.725

^{a)} s.d. = Standard deviation in the overall fit of calculated and experimental complex-formation curves.

better statistical refinement of the polarographic data. In addition, the computed complex-formation curve for different values in the stability constant for $[\text{ML}]^+$ confirmed that it could not be larger than 4.7, otherwise the calculated formation curve would never fit the experimental one. From ESTA refinement, $\log \beta_{\text{CuL}_2}$ varied for different models between 9.2 and 9.7. In the DCP refinement, the value was larger, around 10. If the value of the stability constant for $[\text{CuL}]^+$ was 4.6, then the expected $\log \beta_{\text{CuL}_2}$ value should be *ca.* 9.2 (twice the $\log K_{\text{CuL}}$). This significant difference between GEP and DCP results for $[\text{ML}_2]$ might be due to some influence of adsorption of the ligand on the DCP results in this pH range. In addition, it is possible that the slightly larger GEP value in $\log \beta_{\text{CuL}_2}$ in *Model 1* of *Table 2* is due to the fact that GEP was unable to refine simultaneously both the $[\text{CuL}_2]$ and $[\text{CuL}(\text{OH})]$ stability constants. If one assumes that $[\text{CuL}(\text{OH})]$ is formed to some extent, then the value for $\log \beta_{\text{CuL}_2}$ would be expected to be lower. From the analysis of all the data, it appears that the $[\text{CuL}(\text{OH})]$ species might be formed but in a smaller amount when compared with $[\text{CuL}_2]$. In addition, we verified the formation of $[\text{CuL}(\text{OH})]$ in a similar system, $\text{Cu}^{2+}/\text{TAPSO}/\text{OH}^-$ [7]. The inclusion of the $[\text{CuL}(\text{OH})]$ complex in the model brings the stability-constant value of $[\text{CuL}_2]$ down to a more reasonable value (9.4 ± 0.2) (*Models 3–6, Table 2*).

If $[\text{CuL}(\text{OH})]$ is formed, its stability-constant value of *ca.* 11.5–12.0 (*Models 3–6, Table 2*) is much larger than the expected value from the theoretical point of view, $\log K_{\text{CuL}} + \log K_{\text{MOH}} = 4.6 + 6.1 = 10.7$. It is difficult to justify this value. Similar behavior was described for the system $\text{Cu}^{2+}/\text{TAPSO}/\text{OH}^-$, for which the stability constant of $[\text{ML}(\text{OH})]$ (as $\log \beta$) was found to be 11.43, much larger than the theoretical value, 10.51 [7]. Maybe, the ‘excessively’ large stability constants for $[\text{ML}_2]$ and $[\text{ML}(\text{OH})]$ might be explained by a change in the geometry of the complexes – an attempt is made to grow appropriate crystals.

$[\text{ML}(\text{OH})_2]^-$ does not seem to be formed at all at any significant concentration since it was rejected by ESTA and DCP refinements.

In general, $[\text{CuL}_2(\text{OH})]^-$ was rejected by ESTA, except for *Model 6 (Table 2)* where $[\text{ML}_3]^-$ was fixed. However, $[\text{CuL}_2(\text{OH})]^-$ was readily accepted by DCP refinement (*Model 2, Table 3*) with an overall fit very similar to that obtained for *Model 1* in *Table 3*. The average value from DCP and GEP, $\log \beta_{\text{ML}_2(\text{OH})} \approx 15.6 \pm 1$, is well in the range of the theoretically predicted value ($\log \beta_{\text{CuL}_2} + \log \beta_{\text{Cu}(\text{OH})} = 9.2$ (or

9.6) + 6.1 = 15.3 to 15.7). The large standard deviations associated with the refined stability constants for $[\text{ML}_3]^-$ and $[\text{ML}_2(\text{OH})]^-$ (Model 2, Table 3) were due to the simultaneous refinement of both complexes. It was enough to fix one of them to generate a reasonable standard deviation for the other complex. If $[\text{CuL}_2(\text{OH})]^-$ is formed, it must be a transitional species in a sense that almost immediately the second OH ligand is coordinated to form a very stable complex, $[\text{CuL}_2(\text{OH})_2]^{2-}$ with possibly octahedral configuration. The computed value for this complex is exactly in the expected range ($\log \beta_{\text{CuL}_2} + \log \beta_{\text{Cu}(\text{OH})_2} = 9.2$ (or 9.6) + 11.8 = 21.0 to 21.3), and it suggests that the formation of the $[\text{ML}_2(\text{OH})_2]^{2-}$ complex does not involve a significant change in the geometry of complexes involved. This might suggest that complex $[\text{ML}_2]$ is also octahedral with H_2O or counter-ion molecules in axial positions, and this is why the stability constant of this complex is somewhat larger than expected when compared with the value established for complex $[\text{ML}]^+$. If that supposition holds, then the complex $[\text{ML}_2(\text{OH})]^-$ must also be octahedral with possibly the OH ligand and H_2O (or counter ion) in axial positions. The complex $[\text{CuL}_2(\text{OH})_2]^{2-}$ is a major and 'favorite' species accepted by both refinement operations (potentiometric and polarographic) with computed stability constant of ca. 21.2 ± 0.1 (Tables 2 and 3).

In the GEP refinement, ESTA always refined $[\text{ML}_3]^-$ with a $\log \beta$ very constant (13.53 ± 0.04), indicating that this complex is a predominant species in the solution. A similar value for the stability constant of $[\text{ML}_3]^-$ was obtained from polarography, except for the situation in which $[\text{ML}_3]^-$ and $[\text{ML}_2(\text{OH})]^-$ were refined simultaneously. If complex $[\text{ML}_2(\text{OH})]^-$ is formed, then it coexists with $[\text{ML}_3]^-$ at the same pH (Fig. 4, e and f), and the decrease in the computed stability constant of $[\text{ML}_3]^-$ is expected. If one assumes that $[\text{CuL}_2(\text{OH})]^-$ is formed to some extent, then the range of the value of $\log \beta_{\text{CuL}_3}$ could be 13.3 ± 0.3 , when combining the results obtained from both techniques. If a stability-constant value of, e.g., 13.0 is assumed, then the species-distribution diagram computed for the experimental conditions used for DCP ($[\text{L}_T]/[\text{M}_T] = 155$, $[\text{M}]_T = 4.86 \cdot 10^{-5}$ M) shows that $[\text{ML}_2(\text{OH})]^-$ is a major species in the pH range where $[\text{ML}_3]^-$ coexists (data not shown). However, this observation is not in agreement with the experimental slope of 90 mV/log [L] shown in Fig. 3, b, as well as with the variation in the Z_M function shown in Fig. 2. Next, the stability constant for $[\text{ML}_3]^-$ was adjusted slightly in such a way that the generated calculated complex-formation curves, for which different values of $[\text{ML}_3]^-$ were introduced in the presence of fixed values of $[\text{ML}]^+$, $[\text{ML}_2]$, $[\text{ML}_2(\text{OH})]^-$, and $[\text{ML}_2(\text{OH})_2]^{2-}$, compared well with the experimental complex-formation curve (data not shown). After this exercise, we concluded that the value for $\log \beta_{\text{CuL}_3}$ should be 13.4 ± 0.1 , and this is well within the range of 13.3 ± 0.3 indicated above.

To test the proposed models, species-distribution diagrams were generated for the $[\text{L}_T]/[\text{M}_T]$ ratios 9.1 and 155 (the GEP and DCP exper. conditions, resp.). Fig. 4, a and b, corresponding to the model $[\text{ML}]^+$, $[\text{ML}(\text{OH})]$, $[\text{ML}_3]^-$, and $[\text{ML}_2(\text{OH})_2]^{2-}$, are compatible with Fig. 3, a, but clearly disagree with the experimental results shown in Fig. 2 and Fig. 3, b, where a plateau around 2 for the Z_M function and a slope of 59 mV/log [L], respectively, are well defined. On the other hand, Fig. 4, c and d, suggest that $[\text{ML}]^+$, $[\text{ML}_2]$, $[\text{ML}_3]^-$, and $[\text{ML}_2(\text{OH})_2]^{2-}$ should constitute the most likely model, as it correlates very well with the experimental results presented in Figs. 2 and 3. However, if we assume that both $[\text{ML}_2]$ and $[\text{ML}(\text{OH})]$ are formed, as well as

$[\text{ML}_2(\text{OH})]^-$ (Model 6, Table 2), then two new species-distribution diagrams can be generated (Fig. 4, e and f). The latter, at $[\text{L}_\text{T}]/[\text{M}_\text{T}]$ ratios 9.1 and 155, mainly predict the formation of $[\text{ML}_2]$, $[\text{ML}_2(\text{OH})_2]^{2-}$, and $[\text{ML}_3]^-$, which is in perfect agreement with the main conclusions obtained for the models refined in Tables 2 and 3. Fig. 4, f, suggests a small increase of $[\text{ML}]^+$, without a significant concomitant increase of $[\text{ML}_2]$ in the pH range between 5 and 6.3, which is in agreement with a slight cathodic shift of the potential (Fig. 3, a). Even though $[\text{ML}(\text{OH})]$ and $[\text{ML}_2(\text{OH})]^-$ are present (as minor species), Fig. 4, f, confirms that $[\text{ML}_2]$ and $[\text{ML}_3]^-$ are the predominant species in the pH range where typical slopes of these species were identified (Fig. 3, b).

From the comparison of all reasonable results obtained by GEP and DCP, the model $[\text{ML}]^+$, $[\text{ML}(\text{OH})]$, $[\text{ML}_2]$, $[\text{ML}_2(\text{OH})]^-$, $[\text{ML}_2(\text{OH})_2]^{2-}$, and $[\text{ML}_3]^-$ could be proposed. However, from the considerations above, it is very clear that it is impossible to provide stability constants for all the species with high certainty. The most-certain values were obtained for $[\text{CuL}]^+$, $[\text{CuL}_2]$, $[\text{CuL}_3]^-$, and $[\text{CuL}_2(\text{OH})_2]^{2-}$, and they are, as $\log \beta$, 4.62 ± 0.04 , 9.5 ± 0.1 , 13.4 ± 0.1 , and 21.2 ± 0.1 , respectively. Note that the standard deviations indicate here the ranges in stability constants obtained from different models refined by both techniques. For $[\text{ML}_2]$ and $[\text{ML}_3]^-$, the values were obtained after some iterative processes described above. For the $[\text{CuL}(\text{OH})]$ and $[\text{CuL}_2(\text{OH})]^-$ complexes, only indicative stability constants can be proposed, which are 11.7 ± 0.2 and 15.6 ± 0.2 , respectively. It is also important to mention that $[\text{CuL}]^+$, $[\text{CuL}(\text{OH})]$, and $[\text{CuL}_2(\text{OH})]^-$ are minor and $[\text{CuL}_2]$, $[\text{CuL}_3]^-$, and $[\text{CuL}_2(\text{OH})_2]^{2-}$ are major species formed under the GEP and DCP conditions (Fig. 4, e and f). In Table 4, the final model with the overall stability constants for the $\text{Cu}^{2+}/\text{AMPSO}/\text{OH}^-$ system determined by GEP and DCP are presented.

Table 4. Overall Stability Constants for Copper(II) Complexes with AMPSO Obtained in This Work, after Combining Polarographic and Potentiometric Results. At 25° and 0.1M ionic strength.

Equilibrium	Log β	Equilibrium	Log β
$\text{Cu}^{2+} + \text{L}^- \rightleftharpoons [\text{CuL}]^+$	4.62 ± 0.04	$\text{Cu}^{2+} + \text{L}^- + \text{OH}^- \rightleftharpoons [\text{CuL}(\text{OH})]$	11.7 ± 0.2
$\text{Cu}^{2+} + 2\text{L}^- \rightleftharpoons [\text{CuL}_2]$	9.5 ± 0.1	$\text{Cu}^{2+} + 2\text{L}^- + \text{OH}^- \rightleftharpoons [\text{CuL}_2(\text{OH})]^-$	15.6 ± 0.2
$\text{Cu}^{2+} + 3\text{L}^- \rightleftharpoons [\text{CuL}_3]^-$	13.4 ± 0.1	$\text{Cu}^{2+} + 2\text{L}^- + 2\text{OH}^- \rightleftharpoons [\text{CuL}_2(\text{OH})_2]^{2-}$	21.2 ± 0.1

In the previous work [7], we reported that TAPSO forms six main species with Cu^{2+} : $[\text{CuL}]^+$, $[\text{CuL}(\text{OH})]$, $[\text{CuL}(\text{OH})_2]^-$, $[\text{CuL}_2]$, $[\text{CuL}_2(\text{OH})]^-$, and $[\text{CuL}_2(\text{OH})_2]^{2-}$. The comparison of the models for TAPSO and AMPSO points out, as a major difference, that TAPSO was not able to form $[\text{CuL}_3]^-$. The logical explanation is probably related to the crowded atom arrangement around the N-atom of TAPSO, which does not allow this ligand to form more than $[\text{CuL}_2]$.

Fig. 4, f, shows the species-distribution diagram for the final model proposed, $[\text{CuL}]^+$, $[\text{CuL}(\text{OH})]$, $[\text{CuL}_2]$, $[\text{CuL}_2(\text{OH})]^-$, $[\text{CuL}_2(\text{OH})_2]^{2-}$, and $[\text{CuL}_3]^-$, for the DCP experimental conditions used. This species-distribution diagram shows that AMPSO binds Cu^{2+} strongly, and as a result, the free Cu^{2+} concentration decreases in the presence of $7.5 \cdot 10^{-3}$ M AMPSO from initial $[\text{M}_\text{T}] = 4.9 \cdot 10^{-5}$ M to $3.2 \cdot 10^{-9}$ and $2.4 \cdot 10^{-14}$ M at pH 8.0 and 10.0, respectively. Almost a ten-orders-of-magnitude decrease in the free Cu^{2+} concentration in the pH range where AMPSO is efficient as a buffer can

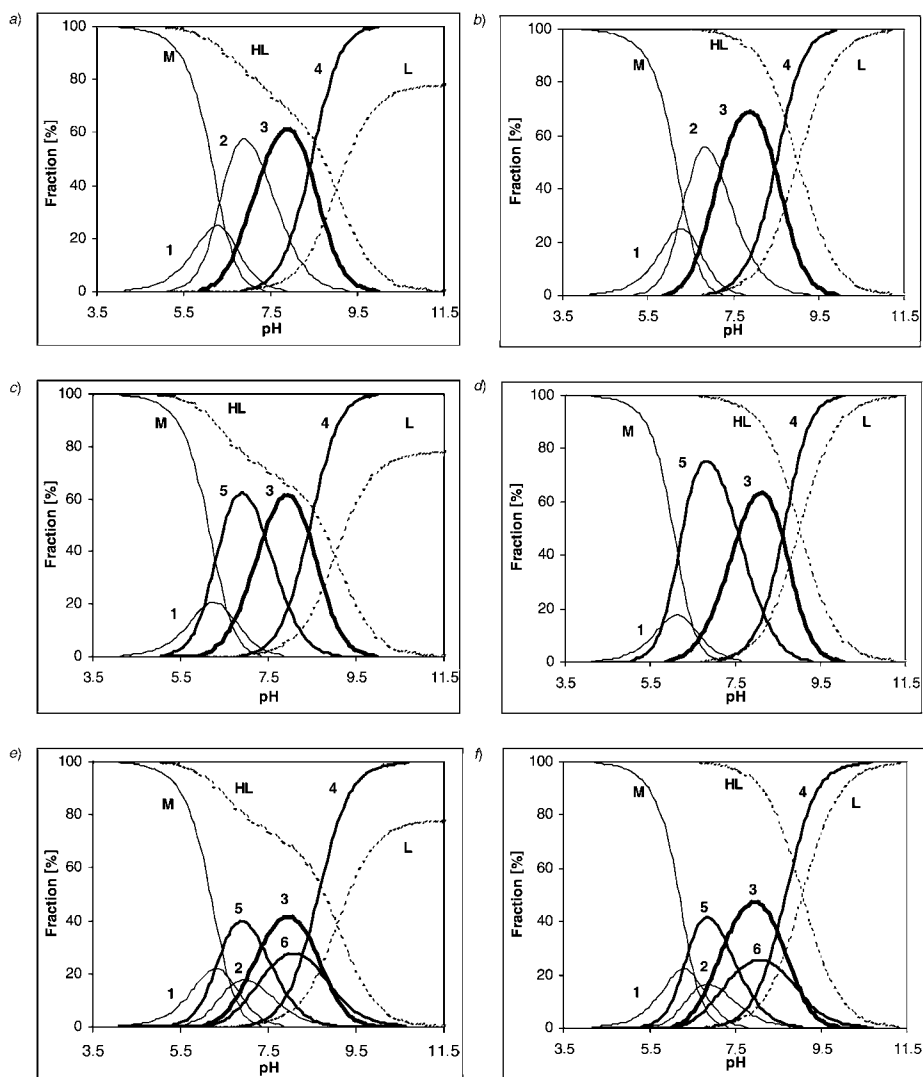


Fig. 4. Species-distribution diagrams computed for different $M/L/OH^-$ models: a) c) e) GEP experimental conditions ($[L_T]/[M_T] = 9.1$, $[M_T] = 8.97 \cdot 10^{-4}$ M); b) d) f) DCP experimental conditions ($[L_T]/[M_T] = 155$, $[M_T] = 4.9 \cdot 10^{-5}$ M). For all $M/L/OH^-$ models, the overall stability constants, as $\log \beta$, are shown: a) b) $[CuL]^+$ (1), $[CuL(OH)]$ (2), $[CuL_3]^-$ (3), and $[CuL_2(OH)_2]^{2-}$ (4), with stability constants set to 4.65, 12.23, 13.51, and 21.35, resp.; c) d) $[CuL]^+$ (1), $[CuL_2]$ (5), $[CuL_3]^-$ (3), and $[CuL_2(OH)_2]^{2-}$ (4), with stability constant set to 4.6, 9.69, 13.51, and 21.33 (c), or 4.62, 9.95, 13.51, and 21.19 (d), resp.; e) f) $[CuL]^+$ (1), $[CuL(OH)]$ (2), $[CuL_2]$ (5), $[CuL_2(OH)]^-$ (6), $[CuL_3]^-$ (3), and $[CuL_2(OH)_2]^{2-}$ (4), with stability constants set to 4.62, 11.7, 9.5, 13.4, 15.7, and 21.2, resp. For sake of simplicity, the charges are omitted in Fig. 4.

be regarded as a huge change. These results should warn the users of *Good* buffers that AMPISO must not be used for studies involving Cu^{2+} ions in solution unless the extent of complexation is accounted for. Taking into account all of what we have stated above,

it is clear that AMPSO forms several strong complexes with Cu^{2+} . Our results disagree entirely with the literature model described by other authors [14] in which only the formation of $[\text{ML}]^+$ was reported.

Stability constants of kinetically labile complexes of amalgam-forming metal ions can be calculated from the dependencies of their DC polarograms. However, it has been shown that when the ligand is specifically adsorbed at the electrode surface, the calculated stability constants differ significantly from the constants obtained by potentiometric measurements [22][23]. It has been proved in this work that, after a simple correction performed on the experimental data, the values of the stability constants determined by DCP, even obtained in the case of a slight adsorption of the ligand at the Hg electrode and a quasi-reversible behavior of the metal ion, are in good agreement with the values obtained by GEP.

In conclusion, this metal/ligand/ OH^- system was a real challenge to model and determine the stability constants. Once again, it was shown that it is very important to use more than one technique to confirm the results; this is even more important when the M/L system is very complicated. As a matter of fact, the analytical techniques employed individually were not able to provide the final model and reliable stability constants. The polarographic technique of speciation and refinement of stability constants employed in this work proved to be as powerful as well-established procedures employed in GEP. We also showed that graphical analysis is very helpful and important, not only in the prediction of the initial model, but also in the verification of the stability constants obtained for the different M/L models considered.

The authors thank the 'Fundação para a Ciência e a Tecnologia' of the Portuguese Government for the financial support of this work, with FEDER funds, with project POCTI/39950/QUI/2001. We also thank Professor *Carlos Gomes* of the Faculty of Sciences, Porto University, for the COPOTISY program.

REFERENCES

- [1] W. J. Ferguson, *Anal. Biochem.* **1980**, *104*, 300.
- [2] N. E. Good, *Biochemistry* **1966**, *5*, 467.
- [3] H. M. V. M. Soares, P. Conde, A. A. N. Almeida, M. T. S. D. Vasconcelos, *Anal. Chim. Acta* **1999**, *394*, 325.
- [4] H. M. V. M. Soares, S. Cardinal, M. G. R. T. M. Barros, *Electroanalysis* **1999**, *11*, 1312.
- [5] H. M. V. M. Soares, P. Conde, *Anal. Chim. Acta* **2000**, *421*, 103.
- [6] H. M. V. M. Soares, M. G. R. T. Barros, *Electroanalysis* **2001**, *13*, 325.
- [7] C. M. M. Machado, P. Gameiro, I. Cukrowski, H. M. V. M. Soares, *Anal. Chim. Acta* **2003**, in press.
- [8] F. J. C. R. Rossotti, H. Rossotti, *J. Chem. Educ.* **1965**, *42*, 375.
- [9] I. Cukrowski, E. Cukrowska, R. D. Hancock, G. Anderegg, *Anal. Chim. Acta* **1995**, *312*, 307.
- [10] H. A. Azab, F. S. Deghaidy, A. S. Orabi, N. Y. Farid, *J. Chem. Eng. Data* **2000**, *45*, 709.
- [11] Z. M. Anwar, H. A. Azab, *J. Chem. Eng. Data* **1999**, *44*, 1151.
- [12] R. N. Roy, L. N. Roy, S. Jordan, J. Weaver, H. Dalsania, K. Kuhler, H. Hagerman, J. Standaert, *J. Chem. Eng. Data* **1997**, *42*, 446.
- [13] Z. M. Anwar, H. A. Azab, *J. Chem. Eng. Data* **2001**, *46*, 34.
- [14] H. A. Azab, A. S. Orabi, E. T. A. El-Salam, *J. Chem. Eng. Data* **2001**, *46*, 346.
- [15] P. M. May, K. Murray, D. R. Williams, *Talanta* **1988**, *35*, 825.
- [16] 'NIST Standard Reference Database 46. NIST Critically Selected Stability Constants of Metal Complexes Database', Version 3.0, data collected and selected by R. M. Smith and A. E. Martell, US Department of Commerce, National Institute of Standards and Technology, 1997.
- [17] I. Cukrowski, *Anal. Chim. Acta* **1996**, *336*, 23.
- [18] I. Cukrowski, M. Adsetts, *J. Electroanal. Chem.* **1997**, *429*, 129.
- [19] E. P. Parry, R. A. Osteryoung, *Anal. Chem.* **1965**, *37*, 1634.

- [20] I. Cukrowski, *J. Electroanal. Chem.* **1999**, 460, 197.
[21] F. Marsicano, C. Monberg, B. S. Martincigh, K. Murray, P. M. May, D. R. Williams, *J. Coord. Chem.* **1988**, 16, 321.
[22] M. Lovric, *Anal. Chim. Acta* **1989**, 218, 7.
[23] E. Casassas, C. Arino, *J. Electroanal. Chem.* **1986**, 213, 235.

Received May 13, 2003